Supporting Information

Nanopillar filters for Surface-Enhanced Raman Spectroscopy

Onur Durucan[1, *], Tomas Rindzevicius[1], Michael Stenbæk Schmidt[1], Marco Matteucci[1], and Anja Boisen[1]

[1]Technical University of Denmark, Department of Micro-and Nano Technology, Kgs. Lyngby, 2800, Denmark

*onurd@nanotech.dtu.dk

Section S1. Experimental Methods

Materials

All chemicals and reagents were used as received. Milk samples (1.5 wt% fat) were acquired from a local grocery, $(CH_3)_2CO$ (99.5 wt%), HCl (32 wt%) and $C_3H_6N_6$ (99 wt%) in powder form were obtained from Sigma-Aldrich. Flat DVD Poly(methyl methacrylate) (PMMA) discs with various thicknesses (0.6 and 1 mm) were purchased from Axxicon. And the 0.14 mm thick pressure sensitive adhesive (PSA) sheets were acquired from ARcare.

Au NP fabrication

The Au NP structures were fabricated on four-inch p-type (100) single side polished Si wafers using previously described maskless lithography technique.[1] According to the standard recipe, 4 min RIE process of Si was followed by 1 min O_2 plasma cleaning procedure. The Cr adhesion layer was not deposited. Thus, Si nanopillar (NP) density was 18 ± 2 pillars/μm^2 with an average height of 390 nm. Further, optimized thickness of Au layer (225 nm) was deposited on etched substrates using electron beam evaporation method. To obtain 4x4 mm^2 SERS chips, unstructured side of Si wafer was scribed via laser micro-machining tool microSTRUCT (3D-Micromac AG) operated at 1064 nm time-bandwidth regime.

Disc Fabrication

A CO_2 laser engraving machine (Epilog Laser) was used to transfer corresponding features on flat PMMA discs. To remove dust particles, PMMA discs were sonicated for 5 min and then rinsed with deionized water. The PSA sheets were processed through electronic cutting tool (Silhouette). PSA was implemented as bonding agent for PMMA layers and SERS chips. Centrifugal microfluidic discs (100 mm in diameter) were obtained by five-layer assembly of patterned PMMA and PSA parts. To achieve sealing between layers, assembled discs were pressed at room temperature under 10 kN bonding force for 1 min. A microfluidic unit in a fabricated disc consists of multiple sections; sample loading chamber, sensing region, waste chamber and capillary channels. A detailed description and visual illustration of disc assembly are included in Figure S1.

Fluidic Experiments

Batch solutions of $C_3H_6N_6$ dissolved in pure milk 100, 200 and 500 ppm were diluted to obtain desired concentrations. The final samples were achieved by consequent addition of 150 µl of $(CH_3)_2CO$ and 50 µl of HCl solutions into 800 µl of milk containing $C_3H_6N_6$. Each addition step was followed by homogenization of the liquid compound using a vortex mixer. The filtration of final analyte suspensions was realized on centrifugal microfluidics platform. Accordingly, 21.5 µl of prepared milk samples were injected into sample loading chambers. Further, the 5 min filtration process was accomplished by controlled rotation of the discs at 47.5 Hz around the predetermined axis using a commercial DC motor RE-35 (Maxon Motors). Lastly, at 25 Hz the liquid was primed to the corresponding waste chamber via capillary channel and the SERS chips were left to dry. The spin stand setup is demonstrated in Figure S1. During the overall microfluidic procedure, the spinning frequency was varied from 0 Hz to 47.5 Hz. The rotational frequency profile for the centrifugal microfluidics procedure is shown in Figure S2.

SERS Measurements

The SERS measurements on dried substrates were carried out using a Thermo Scientific DXRxi Raman microscope with a 10x focusing objective and electron multiplying charge coupled device (EMCCD). The equipment was operated at 780 nm laser wavelength. According to our predetermined exposure parameters; 10 mW laser power and 50 µm aperture size kept constant. Depending on analyte concentration, to avoid the EMCCD saturation, the collection time was varied between 0.01 and 0.05 sec. The chips were mapped over a large area with 25 µm step size. Each Raman spectrum represents an average of 10 acquisitions. The data treatment was performed via a commercial software (MATLAB). Lastly, acquired Raman intensity values were normalized to laser power and exposure time.

Characterization

The morphology of SERS chips after the filtration process was examined using a SEM Zeiss Supra 40 VP. Both contaminated and clean region of the chip were imaged. The microfluidic procedures were visualized using a custom build optical spin-stand setup. The equipment allows to study the fluid behaviour through real-time imaging of the disc during the centrifugation. This is accomplished by a triggering system and high resolution camera pixelfly.PCO (PCO AG) integrated with the motor (Figure S1).

Section S2. Optimization of microfluidics design for wicking-filtration procedure

A functioning design in centrifugal microfluidics platform requires careful optimization of geometrical parameters of capillary channels, chambers, etc. which may affect the fluid behaviour. Moreover, fluidic properties of the sample, centrifugal force and pressure values in the chambers needs to be included in the optimization process. In this study, the presented microfluidic design of discs was developed empirically. Nevertheless, as a starting point, we analytically[2] estimated the desired fluid configuration for the given disc design shown in Figure S3. Thus, we consider the equilibrium condition of centrifugal microfluidic unit during the wicking-filtration stage. The equation of the steady state is given by

$$P_1 + \frac{\rho\omega^2}{2}(h_1)(2r - h_1) = P_0 + \frac{\rho\omega^2}{2}(h_2)(2r - h_2)$$

where P_1 is pressure of compressed air in the sensing chamber; P_0 atmospheric pressure; ρ density of the milk mixture; ω angular frequency of the disc and h_1, h_2 and r are the liquid level heights summarized in Figure S3. At a given rotational frequency (47,5 Hz) and liquid level on the SERS substrate (covering half of the chip), suitable geometrical parameters from above equation were picked to achieve balance in the system. However, in this analytical formula phenomena such as viscosity, sedimentation of the milk and wettability of the liquid towards wells are not considered. Also, the dynamic behaviour of fluid with the change of rotational frequency cannot be evaluated. Therefore, we performed additional step of experimental optimization of the microfluidic disc design via optical imaging system.

Another crucial aspect is related to microfluidics system design. The liquid level management in the sensing chamber (Figure 1d and 1g) is significant for the fluid dynamics of the wicking effect. Firstly, the centrifugal force is radially dependent. Hence, for a reproducible filtration process, the liquid level on the SERS chip should be constant. Moreover, the shape of the liquid front as well as analyte deposition on the SERS substrates will be influenced by the spreading path. Accordingly, we employed the sample handling capabilities of centrifugal microfluidics for accurate immersion of the SERS chip. Even with the adjusted geometry of the disc design, small variations in liquid level may occur due to sample injection method. By pipetting milk mixture into the loading chamber, some liquid may get lost or stuck on the chamber wells. This eventually results in change of liquid levels. We solved this problem by injecting excessive amount of milk mixture (~21.5 µl) where the extra liquid volume is removed in sensing chamber by a valve (Figure S3).

Section S3. Characterization of filtration technique

Direct deposition of a complex sample solution on a SERS substrate is accompanied by nonspecific binding of content on the SERS surface. This, eventually results in blockage of “hot-spots” which has devastating consequence for the SERS signal.[3] To overcome this, we implemented a sample purification method using Au NP substrate as nanofilter and label-free sensing unit at the same time. We verified this approach on a proof-of-concept application: detection of melamine in milk samples.

The surface morphology of the Au NP substrates after the filtration procedure was examined using a Scanning Electron Microscope (SEM). Two distinct regions can be observed: (i) purified and (ii) clogged regions, Figure 5Sa. The “purified” region represents the melamine impregnated area achieved via capillary wicking effect, and the “clogged” (unfiltered) surface part is covered by various solids from milk solution. The interface between

the regions is fixed throughout the filtration process. SEM images show that the unfiltered milk solution is primarily locked to the “clogged” region on the SERS chip while the “purified” part is kept clean, compare Figure S5b with Figures S5c and S5d.

To validate the effectiveness of the filtration and analyte extraction processes, SERS spectra were obtained from both “purified” and “clogged” regions on Au NP substrate using a milk solution containing 50 ppm of melamine, see results in Figure 2. The measurement procedure and signal collection parameters are summarized in Section S1. In Figure 2 statistical data treatment and background correction were not utilized. Two randomly selected melamine SERS spectra recorded from “purified” and “clogged” regions are shown in Figure 2b. In Figure 2a, the SERS map of the “purified” chip surface (~2x4 mm) is presented. The result shows SERS intensity distribution of the characteristic melamine peak at 687 cm^{-1}. The intensity of the Raman mode gradually decreases when approaching the “clogged” region, see the bottom part of the SERS map in Figure 2a. Results indicate that the average SERS intensity of the 687 cm^{-1} mode on the “purified” part is approximately 14 times higher compared to the one obtained from the “clogged” region. The SERS data support our SEM observations and we conclude that contaminants blocking the SERS signal are successfully withhold in the ’Clogged’ region.

Supporting Videos

Video S1: Real-time video record of centrifugal microfluidic disc unit during the rotation. The images for the video were captured using the optical spin stand setup. The general process of liquid manipulation in centrifugal platform are shown step by step.

Video S2: Magnified video record of SERS chip during the wicking based nanofiltration step. Tiny liquid layer which spreads on the SERS substrate from the immersion boundary can be observed by comparing contrasts of different regions on substrate surface.

Supporting Figures

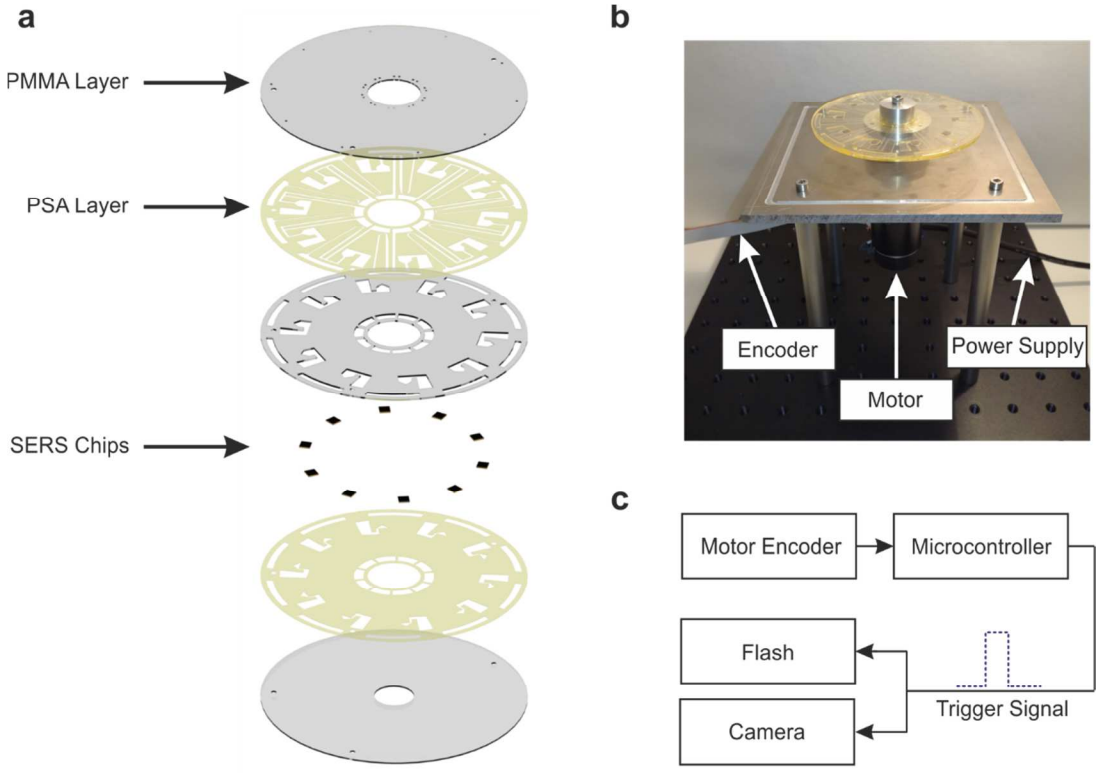

Figure S1: a) Schematic representation of disc assembly. Processed poly(methyl methacrylate) (PMMA) parts, pressure sensitive adhesive (PSA) layers and surface-enhanced Raman spectroscopy (SERS) chips are alternately joined to obtain centrifugal microfluidic system for the filtration procedure. Three pinholes on each PMMA and PSA layers were utilized to align parts during the assembly of the disc. b) Spin stand setup for the centrifugal microfluidics. A programmable motor was employed to execute microfluidic procedures. The encoder of the motor provides the angular position of microfluidic disc which was used for imaging during the rotation. c) Chart flow of optical imaging system for the spin stand. Electrical signal from the encoder is processed by the microcontroller to synchronize and generate appropriate trigger pulses for the camera and flash light.

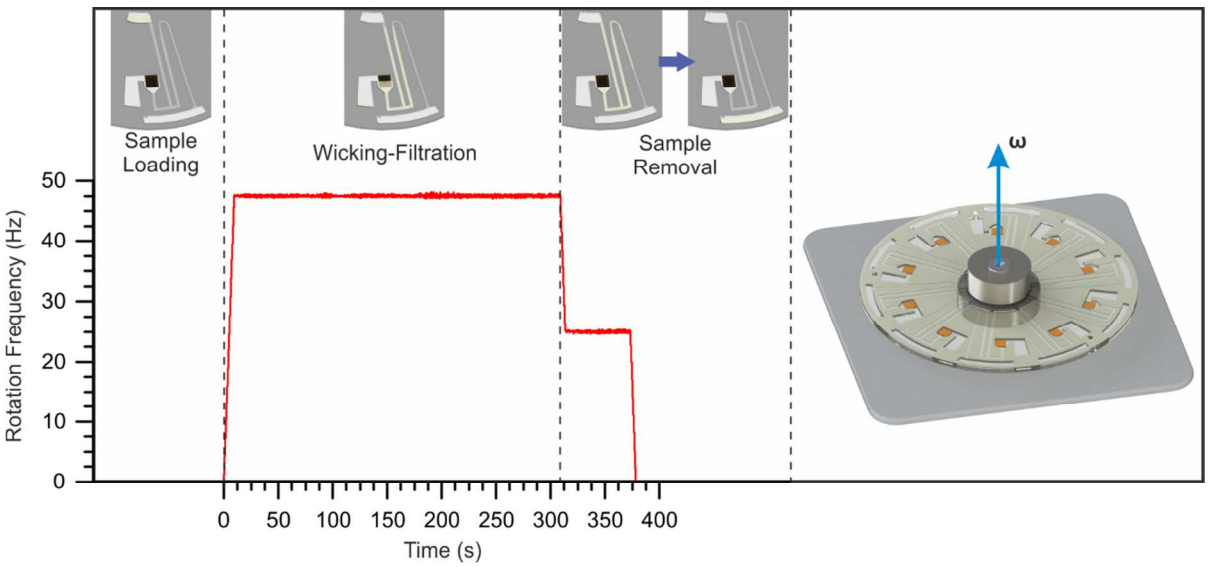

Figure S2: With the help of centrifugal force and pneumatic chamber, injected milk samples are transferred into desired chambers. Spin stand integrated with the encoder allows to control the rotation frequency of the disc which is crucial to perform reproducible wicking-filtration processes and liquid manipulations. In this graph, three steps of microfluidic procedure and corresponding frequency profile are depicted.

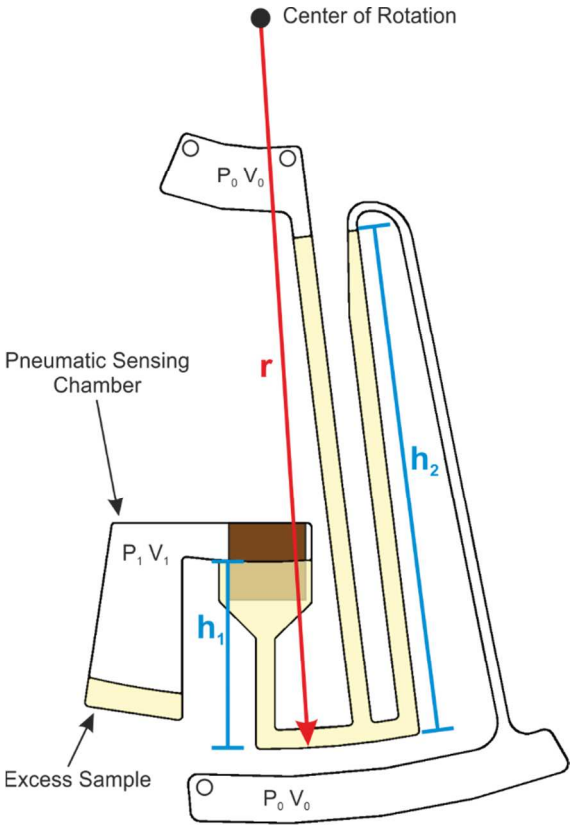

Figure S3: The optimized geometry of pneumatic sensing chamber and fluid dynamics of the centrifugal system was utilized to preserve liquid level (h_1) on SERS chip. This eventually realized by allowing “excess sample” to overflow above the well in sensing chamber. The configuration of microfluidic system at equilibrium condition is defined by radial distances of liquid levels, pressure in the chambers, characteristic properties of the fluid and the rotational frequency.

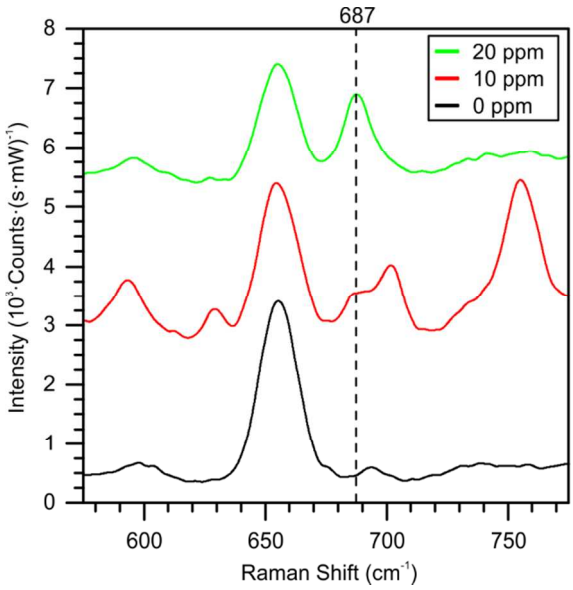

Figure S4: Sample mixture containing 10 and 20 ppm of melamine are compared with the pure control milk solution. The peak arising at 687 cm^{-1} is clearly indicating the presence of milk contaminant.

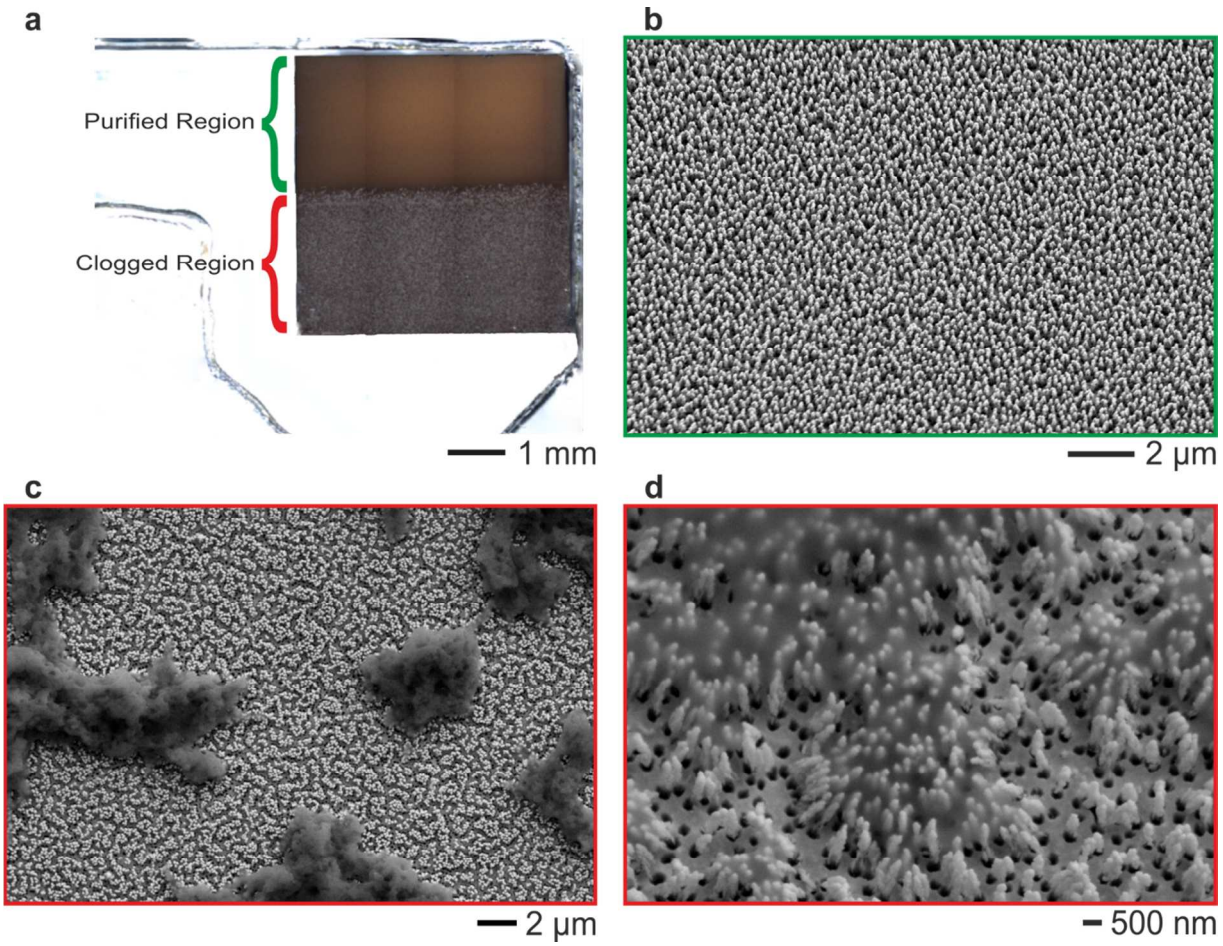

Figure S5: a) An optical microscope image of a sensing chamber. Depending on the type of liquid transport (capillary wicking or immersion), the SERS chip is divided into “Purified” and “Clogged” regions respectively. b) SEM image acquired from the “Purified” region. c) SEM image from the “Clogged” region. d) A magnified SEM image from the same area as in (c).

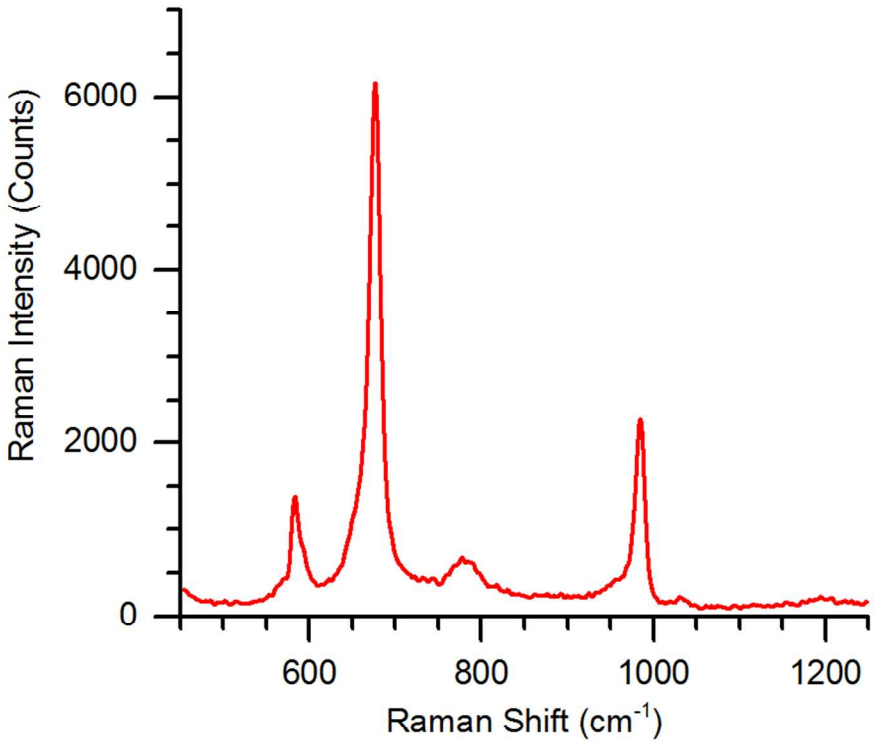

Figure S6: Raman spectrum of pure melamine in powder form.

REFERENCES

(1) Wu, K.; Rindzevicius, T.; Schmidt, M. S.; Mogensen, K. B.; Hakonen, A.; Boisen, A. Wafer-Scale Leaning Silver Nanopillars for Molecular Detection at Ultra-Low Concentrations. *J. Phys. Chem. C* **2015**, *119*, 2053–2062.

(2) Ducrée, J.; Haeberle, S.; Lutz, S.; Pausch, S.; Stetten, F. Von; Zengerle, R. The Centrifugal Microfluidic Bio-Disk Platform. *J. Micromechanics Microengineering* **2007**, *17*, S103–S115.

(3) Sun, F.; Hung, H.; Sinclair, A.; Zhang, P.; Bai, T.; Galvan, D. D.; Jain, P.; Li, B.; Jiang, S.; Yu, Q. Hierarchical Zwitterionic Modification of a SERS Substrate Enables Real-Time Drug Monitoring in Blood Plasma. *Nat. Commun.* **2016**, *7*, 13437.